Dynamic regulation of *eve* stripe 2 expression reveals transcriptional bursts in living *Drosophila* embryos

Jacques P. Bothma[a,1], Hernan G. Garcia[b,1], Emilia Esposito[a], Gavin Schlissel[a], Thomas Gregor[b,c,2], and Michael Levine[a,2]

[a]Department of Molecular and Cell Biology, University of California, Berkeley, CA 94720; and [b]Joseph Henry Laboratories of Physics and [c]Lewis-Sigler Institute for Integrative Genomics, Princeton University, Princeton, NJ 08544

Contributed by Michael Levine, May 30, 2014 (sent for review April 9, 2014; reviewed by William McGinnis and Scott Barolo)

We present the use of recently developed live imaging methods to examine the dynamic regulation of *even-skipped* (*eve*) stripe 2 expression in the precellular *Drosophila* embryo. Nascent transcripts were visualized via MS2 RNA stem loops. The *eve* stripe 2 transgene exhibits a highly dynamic pattern of de novo transcription, beginning with a broad domain of expression during nuclear cycle 12 (nc12), and progressive refinement during nc13 and nc14. The mature stripe 2 pattern is surprisingly transient, constituting just ∼15 min of the ∼90-min period of expression. Nonetheless, this dynamic transcription profile faithfully predicts the limits of the mature stripe visualized by conventional in situ detection methods. Analysis of individual transcription foci reveals intermittent bursts of de novo transcription, with duration cycles of 4–10 min. We discuss a multistate model of transcription regulation and speculate on its role in the dynamic repression of the *eve* stripe 2 expression pattern during development.

The *Drosophila even-skipped* (*eve*) stripe 2 enhancer is one of the best-characterized *cis*-regulatory DNAs in animal development (1). A combination of genetic analyses, DNA binding assays, and site-directed mutagenesis led to a detailed model for the regulation of stripe 2, whereby the maternal Bicoid gradient, in concert with zygotic Hunchback protein, defines a broad domain of activation in the anterior half of the embryo (2–5). Localized gap repressors, Giant in anterior regions and Kruppel in central regions, establish the anterior and posterior stripe borders, respectively (summarized in Fig. 1*A*).

Most of our information regarding the regulation of the stripe 2 expression pattern is derived from the analysis of fixed preparations of staged embryos (2, 5, 6). Here, we use a newly developed live-imaging technique (7, 8) to explore the detailed temporal dynamics of the *eve* stripe 2 expression pattern in living embryos. Multiple copies of an MS2 stem loop sequence were inserted into the 5′-UTR of a *yellow* reporter transgene (Fig. 1*B*). The loops form upon transcription by RNA polymerase II (Pol II) and are bound by a maternally provided MS2 coat protein fused to GFP (MCP-GFP) (9–14). As a result, fluorescence signals are detected at sites of Pol II elongation and de novo transcription, and the strength of the signals are proportional to the number of elongating Pol II complexes (7).

This method was recently used to examine the activation of the proximal *hunchback* enhancer by the Bicoid gradient in the anterior half of the precellular embryo (7, 8). Diminishing levels of Bicoid were shown to cause stochastic on/off transcription of the *hunchback*>MS2 transgene at the posterior limits of the Hunchback expression pattern. This observation suggests that the Bicoid activator not only augments the levels of transcription but also increases the probability that a given cell within a population will initiate expression (15).

The regulation of the *hunchback*>MS2 transgene is rather static. Once activated by Bicoid during nuclear division cycle 10 (nc10) (16), the spatial features of the pattern remain essentially constant for the next hour until transcription is lost at the midpoint of nc14 (7, 17). In contrast, the *eve* stripe 2 pattern is highly dynamic, with broad activation during nc11 and nc12, followed by progressive refinement during nc13 and nc14 (4). These regulatory dynamics are nicely captured by the MS2 detection system and reveal surprisingly transient expression of the mature stripe (Fig. 1*D* and Movie S1). We also present evidence for the occurrence of sporadic transcriptional bursts, with fluctuation cycles of 4–10 min. We discuss the possibility that these discontinuities in de novo transcription facilitate the dynamic regulation of *eve* stripe 2 expression by the localized Giant and Kruppel repressors.

Results

The first 1.7 kb of the *eve* 5′ flanking region was attached to a *yellow* reporter gene containing 24 tandem repeats of the 60- to 70-bp MS2 stem loop motif [summarized in Fig. 1*B* (18)]. The *eve*>MS2 fusion gene contains the "full-length" 720-bp *eve* stripe 2 enhancer, located between –1.5 kb and –800 bp upstream of the *eve* transcription start (4, 19). It also contains dispersed regulatory sequences that mediate weak expression within the limits of stripe 7 (Fig. 1*C*). Conventional in situ hybridization assays identify authentic stripe 2 and stripe 7 expression patterns, as seen for similar *eve* reporter genes lacking MS2 stem loop sequences (e.g., refs. 20 and 21), confirming that the presence of the stem loops does not significantly affect the output pattern of expression.

Dynamics of Stripe Formation. The *eve*>MS2 transgene was introduced into embryos containing a maternally expressed MCP-GFP fusion protein, as described in ref. 7. Sites of de novo transcription were imaged by sampling a series of confocal *z*

Significance

There is considerable information about the spatial regulation of gene expression during pattern formation in animal development. Significantly less is known about temporal control, in part due to our inability to analyze gene activity in real time. Using a recently developed approach for the visualization of gene expression in living *Drosophila* embryos, we examined the well-known *even-skipped* stripe 2 expression pattern. Surprisingly, we observe that this classic pattern is quite transient and generated by discontinuous surges of transcriptional activity in individual cells. These results challenge a purely static framework for dissecting developmental programs and emphasize the importance of the dynamic features of pattern formation.

Author contributions: J.P.B., H.G.G., E.E., G.S., T.G., and M.L. designed research, performed research, contributed new reagents/analytic tools, analyzed data, and wrote the paper.

Reviewers: W.M., University of California, San Diego; and S.B., University of Michigan Medical School.

The authors declare no conflict of interest.

Freely available online through the PNAS open access option.

[1]J.P.B. and H.G.G. contributed equally to this work.

[2]To whom correspondence may be addressed. Email: mlevine@berkeley.edu or tg2@princeton.edu.

This article contains supporting information online at www.pnas.org/lookup/suppl/doi:10.1073/pnas.1410022111/-/DCSupplemental.

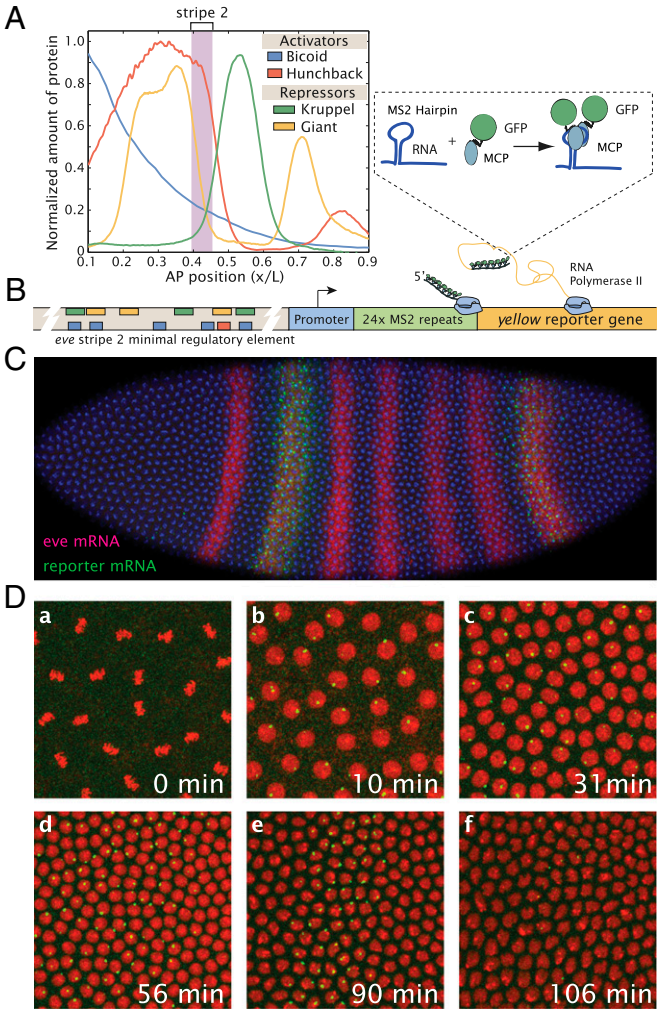

Fig. 1. Live imaging of *eve* stripe 2 transcriptional activity. (*A*) Schematic representation of *eve* stripe 2 regulation (data from refs. 38 and 39). The stripe is the result of the combined activation of Bicoid and Hunchback, which define a broad activation domain in the anterior part of the embryo, and repressors Giant and Kruppel, which restrict expression anterior and posterior of this domain, respectively (4). (*B*) Structure of the reporter construct: the *eve* stripe 2 DNA region (−1.7 kbp, +50 bp) was placed upstream of 24 repeats of the MS2 stem loops and a *yellow* reporter gene. The MCP-GFP protein that binds to these stem loops is present in the unfertilized egg and in the early embryo. (*C*) Confocal image of a transgenic embryo carrying the *eve*>MS2 transgene labeled via in situ hybridization with full-length probes for the *yellow* reporter gene (plasmid transgene) and endogenous *eve* RNAs in the same embryo during nc14. (*D*) Projected confocal stack of a live *Drosophila* embryo at six time points (*a*–*f*) centered at ∼40% embryo length, expressing the *eve*>MS2 transgene, histone RFP (red), and MCP-GFP (green). Each image is 77 μm × 77 μm. (*a*) At metaphase of nc11, no foci of transcription are detectable. (*b*) Same embryo 10.3 min later than *a* during nc12 interphase. There are clear fluorescent foci indicating sites of nascent transcript formation. (c) Embryo in nc13 interphase showing broad expression of the transgene. (*d*) At the onset of nc14, the stripe pattern has started to refine. (e) Refined stripe by late nc14. (*f*) Embryo just before gastrulation when the transgene expression has diminished significantly.

sections through the entirety of cortical nuclei. The fluorescence intensities of these expression puncta is a proxy for the number of Pol II molecules actively transcribing the reporter gene and hence is an instantaneous measure of activity (7). A broad spatial domain of transcriptional activity is detected during nc11, nc12, and nc13 (e.g., Fig. 1 *D*, *a*–*c* and Movies S1–S3). The stripe is gradually refined during nc14 (Fig. 1 *D*, *d* and *e*), and ultimately disappears before the onset of gastrulation (Fig. 1 *D*, *f*; see below). The dynamics of the stripe 2 expression pattern, broad activation followed by localized repression, is consistent with previous studies of fixed embryos (e.g., ref. 4). As observed in classical studies (e.g., ref. 22), there is no evidence of transcription during mitosis (e.g., Fig. 1 *D*, *a*).

There is a marked restriction in the posterior limits of the reactivated expression pattern following the mitosis at nc13/nc14 (Movies S2 and S3). During nc13, de novo transcription is observed throughout most of the length of the embryo, spanning 10–70% along the anterior-posterior (AP) limits of the embryo. However, at the onset of nc14, the transgene is reactivated within tighter spatial limits, from 20% to 50% across the AP axis. This initial nc14 pattern is broader than the final limits of the mature stripe, but considerably more restricted than the pre-nc14 pattern (Movies S2 and S3).

The progressive refinement of the mature stripe 2 expression pattern (Fig. 2 *A*–*C*) is revealed by quantifying the instantaneous fraction of nuclei exhibiting fluorescent signals of de novo transcription. There is relatively uniform activation of *eve*>MS2 transcription within a broad domain centered at 40% embryo length of nc13 embryos, This pattern is refined into the mature stripe during a 20-min window of nc14 (Fig. 2*D*, dashed line), but quickly disappears before the onset of gastrulation (Fig. 2*E*). The mature stripe 2 pattern is far more transient than the picture formed from conventional in situ hybridization assays using fixed embryos (e.g., refs. 20 and 21).

Dynamic Regulation Predicts the Mature Expression Pattern. Image analysis methods were used to quantify the signal intensities of individual transcription foci in an effort to understand how the dynamic de novo transcription profile produces a steady-state stripe of expression (7). Signal intensities were tracked for individual nuclei during the entirety of nc14 development. Some of these nuclei reside within the limits of the mature stripe, whereas others are located just beyond the anterior and posterior borders of the stripe (Fig. 3*A*). Interestingly, there is an overall reduction of signal intensities within the stripe 2 domain at the midpoint of nc14 (arrow, Fig. 3*A*). This transient reduction might reflect a change in the regulatory landscape, for example, due to the accumulation of Giant and Kruppel repressors as the mature stripe is formed. A similar reduction in expression was observed for the *hunchback*>MS2 transgene at ∼12 min after onset of nc14 (7).

By integrating fluorescent traces over time, we calculated the spatial profile of mRNAs produced per nucleus at each time point during nc14 (Fig. 3 *B*–*D*, *SI Text*, and Movie S4) (7). The mature stripe of steady-state mRNAs becomes apparent at ∼30 min into nc14, when each nucleus produces ∼130 mRNAs (*SI Text*). To systematically quantify the width of the stripe, a Gaussian curve was fitted to the mRNA accumulation profiles at the end of nc14 (Fig. 3*D*). This analysis reveals a mature stripe that is centered at 41.0 ± 0.1% egg length with half-maximum at full-width limits of 5.3 ± 0.1% egg length. The stripe position is entirely consistent with previous reports based on in situ hybridization assays and antibody staining of fixed embryos (located between 39% and 43% egg length; see ref. 23).

As mentioned above, the de novo transcription profiles predict the final limits of the mature stripe 2 pattern (Figs. 2*C* and 3*C*) as visualized by conventional methods (Fig. 1*C*). Thus, posttranscriptional mechanisms, such as differential mRNA stability, are unnecessary to account for the dynamics of the stripe 2 expression pattern. However, mRNA half-life does affect the total number of steady-state mRNAs and proteins present within the stripe. When we assume a half-life of ∼7 min, as measured for *ftz* mRNAs (24), the position and width of the stripe remains unchanged, but there is a reduction in the total

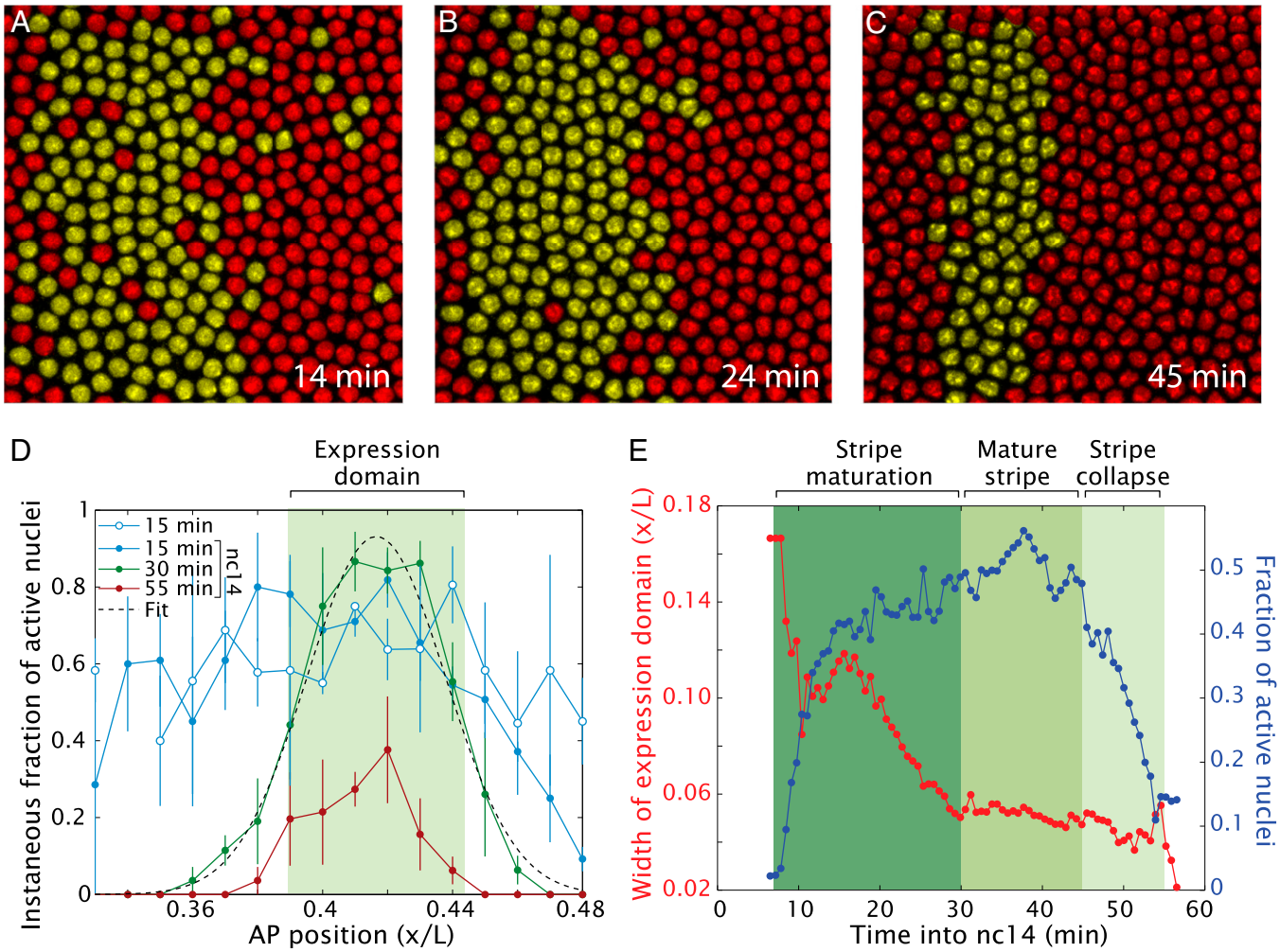

Fig. 2. Formation and refinement of stripe 2 expression domain. (*A*–*C*) Snapshots of a *Drosophila* embryo expressing the *eve*>MS2 reporter at different times in nc14 centered at ~37% embryo length. Nuclei that show foci of active transcription have been false-colored yellow. (*D*) Instantaneous fraction of active nuclei as a function of position in nc13 and at different times during nc14. The expression domain is defined as the area within the full width at half-maximum of a Gaussian fit to the profile at each time point. (*E*) Expression domain width and fraction of active nuclei within the domain as a function of time obtained from Gaussian fits as shown in *D*. After entry into nc14, the width of the domain refines and the fraction of active nuclei within it increases. The mature stripe is stable for 15 min and decays rapidly as gastrulation approaches. The temporal progression of the spatial profile of the fraction of active nuclei is also shown in Movie S5. (All data were obtained by averaging over four embryos; error bars correspond to SEMs.)

number of steady-state mRNAs (Fig. 3*E* and Movie S5). Furthermore, assuming a protein translation rate of one protein per mRNA per min (25) and a protein half-life of 6–40 min (26), we predict an average of ~1,200 Eve proteins per nucleus within the mature stripe 2 domain. It should be possible to test these predictions using quantitative in situ detection methods.

Bursts of Transcriptional Activity in Individual Nuclei. The preceding analysis reveals a highly dynamic pattern of de novo transcription. In an effort to gain insights into the underlying mechanisms, we measured the fluorescence intensities of individual foci during the entirety of nc14. There are significant oscillatory fluctuations in fluorescence signal intensities during nc14 (Fig. 4*A* and Fig. S2). A typical nucleus within the definitive stripe 2 domain displays reactivation of de novo transcription within ~10 min after the onset of nc14. There are variable reductions in the levels of transcription followed by surges or bursts of expression. These fluctuations are evocative of transcriptional bursts reported in a number of other systems subject to live-image analysis, including bacteria, yeast, *Dictyostelium*, and cultured mammalian cells (18). Moreover, previous analysis based on fixed *Drosophila* embryos found evidence of transcriptional bursting at the Hox gene *Scr* (27) and in gap gene expression (17).

Transcriptional "bursts" have been associated with promoters that switch between ON and OFF states (28, 29). In this simple "two-state model," transcription occurs only when the promoter is in the ON state and no transcription is permitted when the promoter is in the OFF state (summarized in Fig. 4*B*). To determine whether this simple model can describe the fluctuations of *eve* transcription, we calculated the dynamics of Pol II loading based on the fluorescence signal intensities at individual sites of de novo transcription. These signals are a proxy for the number of Pol II molecules actively transcribing the gene (Fig. 4 *A* and *C*). Changes in signal intensities can be directly related to the rate of Pol II loading at the promoter (Fig. 4 *D* and *E*) using a previously described model (7) (*SI Text*). We observed highly variable burst cycles of 4–10 min, and the production of 20–100 mRNAs per typical burst (Fig. 4 *A* and *E*, and Fig. S2). Both the time of persistence and the number of mRNAs produced per burst are comparable to those observed in other systems using similar live-imaging methods as well as fixed tissue techniques (10, 11, 28, 30). Surprisingly, however, these bursts

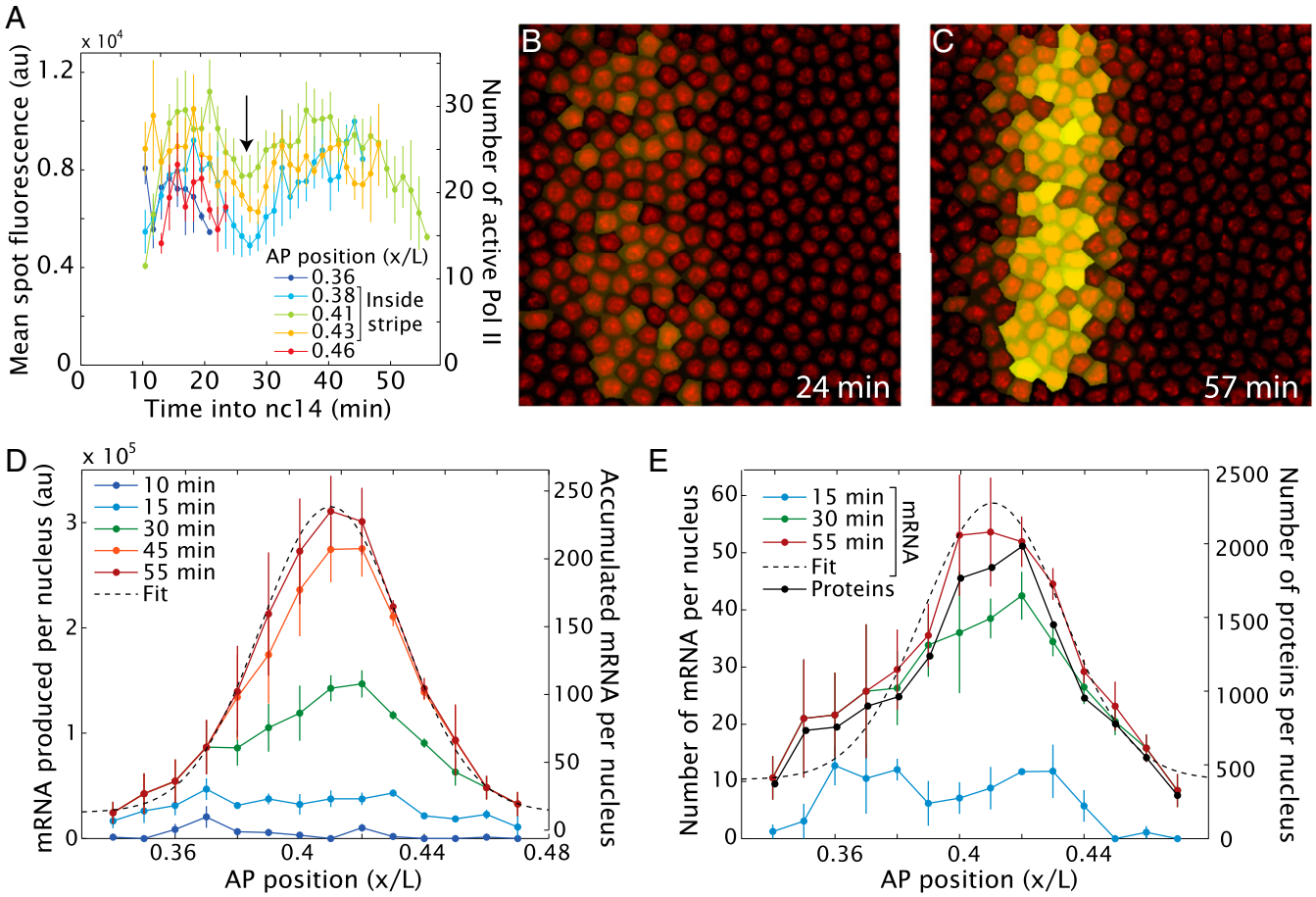

Fig. 3. Dynamics of *eve* stripe 2 mRNA distribution. (*A*) Mean spot fluorescence, indicating transcriptional activity, as a function of time for different positions along the AP axis of the embryo. The arrow indicates a reduction in the average fluorescence that consistently occurs at about 28 min into nc14 in all embryos observed. (*B* and *C*) By integrating the total fluorescence as a function of time and assuming no mRNA degradation, it is possible to predict the amount of accumulated mRNA (*SI Text*). The intensity of the yellow false-color label is proportional to the amount of mRNA produced in each nucleus. (*D*) Total amount of mRNA produced per nucleus, assuming no degradation as a function of position along the AP axis at different time points during nc14. The absolute number of mRNA molecules should be seen as an estimate (*SI Text*). (*E*) Number of mRNA and protein molecules per nucleus assuming an *eve* mRNA half-life of 7 min (24), a protein translation rate of one protein per mRNA per min (25) and a protein half-life of 6–40 min (26). The exact half-life of *eve* mRNA that is used for this model has little influence on the qualitative appearance of the stripe (Fig. S1 and Movie S4). The temporal progression of all parameters is shown in Movie S5. (All data were obtained by averaging over four embryos; error bars correspond to SEMs.)

do not present a single characteristic rate of Pol II loading but correspond to discrete values ranging from a peak of 14 elongating Pol II complexes per min to a minimum of 4 Pol II per min.

The occurrence of multiple rates of Pol II loading argues against a simple two-state model of transcription (Fig. 4*B*). Instead, the data are consistent with a "multistate model," with promoter switching between several discrete transcriptional states (Fig. 4*B* and Fig. S2). For both the multistate model and the simpler two-state model, the molecular mechanisms underlying these multiple transcriptional states are uncertain (see below).

Discussion

During the past 30 years, we have obtained a comprehensive picture of the spatial patterning processes underlying the segmentation of the *Drosophila* embryo [e.g., reviewed by Levine (1)]. However, considerably less is known about the temporal dynamics of this process. Here, we applied recently developed live-imaging methods to monitor the transcriptional activity of an *eve* stripe 2 fusion gene in living *Drosophila* embryos. We found that the mature *eve* stipe 2 expression pattern is surprisingly short-lived and persists for only ~15 min after it is fully formed (Fig. 2). Nonetheless, the temporal dynamics of de novo transcription accurately account for the steady-state expression of *eve* stripe 2 seen with conventional in situ detection methods (Fig. 3). A critical observation of this study is the occurrence of transcriptional bursts underlying the dynamic *eve* expression pattern. These bursts are highly variable in duration and in mRNA output, and a simple two-state model cannot explain them (Fig. 4).

The ephemeral nature of the stripe 2 expression pattern highlights our ignorance of the temporal dynamics of the segmentation gene network, despite extensive insights into the spatial control of expression (e.g., ref. 1). Timing is just as important for developmental fate decisions as the control of the spatial limits, and it is now possible to measure the temporal control of gene expression using newly developed live-imaging methods (7, 8). Indeed, recent evidence suggests that promoters with poised Pol II exhibit more rapid activation dynamics than those lacking poised Pol II, and subtle differences in the timing of expression can influence the coordination of cell invagination events during gastrulation (31).

Previous live-imaging studies have reported transcription bursts, whereby promoters switch between ON and OFF states (10, 11, 28, 30) (Fig. 4*B*). Such bursts have also been inferred

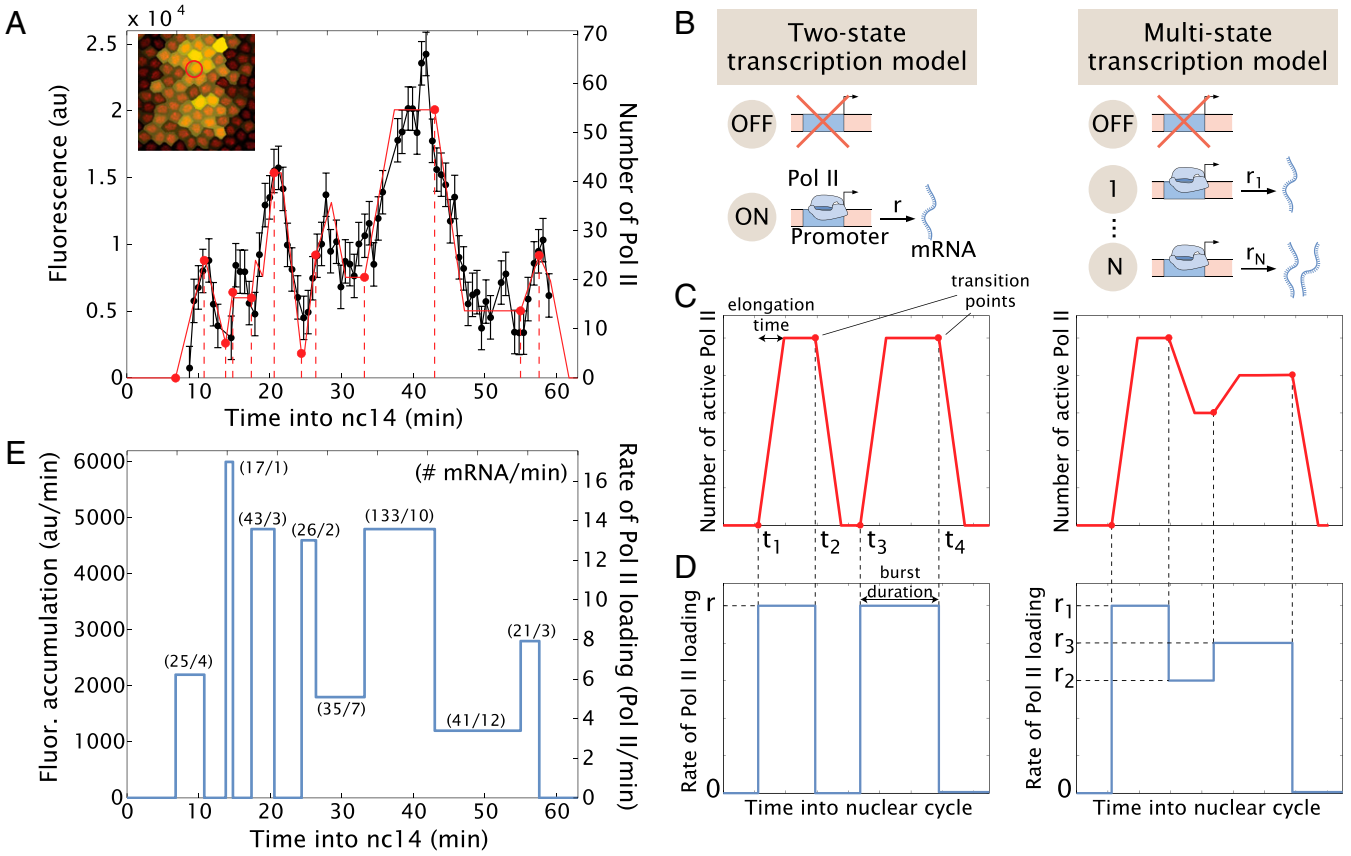

Fig. 4. Transcriptional bursting in *eve* stripe 2 activity. (*A*) Fluorescence intensity of an individual spot within the stripe (black) and manual fits consistent with the simple model put forth in *B–D* (red); error bars are imaging errors as in Garcia et al. (7). *Inset* (51 μm × 51 μm) shows the nuclear location corresponding to the spot using false coloring as in Fig. 3*C*. (*B*) The widespread two-state model of transcription posits that promoters can be in an OFF or ON state. Transcription factors can then regulate the rates of interconversion between these two states or the rate of transcriptional initiation in the ON state. In a more general multistate model of transcription, the promoter can be found in the OFF state as well as several ON states, each one of which has a characteristic rate of transcription initiation, i.e., polymerase loading rate. (*C*) The strength of *eve*>MS2 fluorescent foci are proportionate to the number of elongating Pol II complexes across the gene template. (*D*) The rate of Pol II loading is related to the spot fluorescence intensity through the time Pol II molecules spend bound to the gene during transcript elongation. Two example time traces of the rate of Pol II loading and their corresponding fluorescence dynamics are shown. In the example for the two-state model, Pol II molecules are loaded onto the gene at a rate r starting at a time t_1 after mitosis resulting in a linear increase of fluorescence. Once the first Pol II molecule reaches the end of the gene and falls off [~4.2 ± 0.4 min; see Garcia et al. (7)], the number of Pol II molecules on the gene will reach steady state, resulting in a constant fluorescence value. At time t_2, the promoter is switched OFF and the fluorescence intensity will decline as Pol II molecules terminate transcription. (*E*) Estimated rate of Pol II loading resulting from the manual fits in *A*. The estimated number of mRNA molecules produced per state and their duration are shown.

from fixed embryo data (17, 27). However, our analysis of *eve* stripe 2 regulation suggests a more nuanced picture of the transcription dynamics. We find evidence for multiple ON states, with each state exhibiting a distinct rate of Pol II loading and release from the *eve* promoter. Because the nc14 interphase occurs after DNA replication, there are two copies of each allele on adjoining sister chromatids. Independent burst cycles from each copy could contribute to the observed multistate complexity. Additional molecular mechanisms underlying promoter switching include occupancy of transcription factor binding sites, nucleosome remodeling, disassembly of the preinitiation complex, and stochastic enhancer-promoter looping events (32–35).

It is possible that transcriptional bursting could contribute to the dynamic regulation of the *eve* stripe 2 expression pattern. In the critical region of refinement, there are overlapping distributions of activators (Bicoid and Hunchback) and repressors (Giant and Kruppel). At the beginning of nc14, the activators have the upper hand and it is only as the concentration of Giant and Kruppel increase that the pattern becomes refined (36). Perhaps the "OFF phase" of the *eve* bursts is particularly susceptible to repression during this increase in the levels of Giant and Kruppel. The OFF phase might reflect the uncoupling of the stripe 2 enhancer and transcriptional machinery, thereby rendering the enhancer DNA more accessible to the newly synthesized repressors (e.g., ref. 37). The *hunchback*>MS2 transgene exhibits a relatively static pattern of expression (7, 8), and it is currently unclear whether individual nuclei exhibit transcriptional bursting behaviors.

It remains to be seen whether the transcriptional bursts or surges identified in this study are a general property of gene expression in the *Drosophila* embryo, or a property of dynamically regulated genes such as *eve*. It is striking that *eve* transcription is stochastic and discontinuous because the *Drosophila* syncytium exhibits the most rapid regulatory dynamics known in animal development. Future studies will explore the possibility that previously described mechanisms of transcriptional precision, e.g., paused Pol II and shadow enhancers (e.g., ref. 37), somehow suppress transcriptional bursts to produce more uniform rates of mRNA synthesis.

Methods

Female virgins maternally expressing MCP-GFP and Histone-RFP from ref. 7 were crossed with males of the *eve*>MS2-yellow reporter line. Collected embryos were imaged using either two-photon or confocal microscopy. At each time point, a stack of at least 10 images separated by 0.5 μm (confocal) or 1 μm (two-photon) was acquired. MCP-GFP spots are detected, their fluorescence is quantified in 3D (7), and they are assigned to the closest segmented nucleus. See *SI Methods* for details on transgenic fly construction, sample preparation, and data acquisition and analysis.

ACKNOWLEDGMENTS. This work was supported by National Institutes of Health Grants R01 GM34431 (to M.L.), P50 GM071508 (to T.G.), and R01 GM097275 (to T.G.), and by Searle Scholar Award 10-SSP-274 (to T.G.). H.G.G. holds a Career Award at the Scientific Interface from the Burroughs Wellcome Fund and a Princeton Dicke Fellowship.

1. Levine M (2010) Transcriptional enhancers in animal development and evolution. *Curr Biol* 20(17):R754–R763.
2. Small S, Kraut R, Hoey T, Warrior R, Levine M (1991) Transcriptional regulation of a pair-rule stripe in *Drosophila*. *Genes Dev* 5(5):827–839.
3. Stanojevic D, Small S, Levine M (1991) Regulation of a segmentation stripe by overlapping activators and repressors in the *Drosophila* embryo. *Science* 254(5036): 1385–1387.
4. Small S, Blair A, Levine M (1992) Regulation of *even-skipped* stripe 2 in the *Drosophila* embryo. *EMBO J* 11(11):4047–4057.
5. Arnosti DN, Barolo S, Levine M, Small S (1996) The *eve* stripe 2 enhancer employs multiple modes of transcriptional synergy. *Development* 122(1):205–214.
6. Surkova S, et al. (2008) Characterization of the *Drosophila* segment determination morphome. *Dev Biol* 313(2):844–862.
7. Garcia HG, Tikhonov M, Lin A, Gregor T (2013) Quantitative imaging of transcription in living *Drosophila* embryos links polymerase activity to patterning. *Curr Biol* 23(21): 2140–2145.
8. Lucas T, et al. (2013) Live imaging of bicoid-dependent transcription in *Drosophila* embryos. *Curr Biol* 23(21):2135–2139.
9. Bertrand E, et al. (1998) Localization of ASH1 mRNA particles in living yeast. *Mol Cell* 2(4):437–445.
10. Golding I, Paulsson J, Zawilski SM, Cox EC (2005) Real-time kinetics of gene activity in individual bacteria. *Cell* 123(6):1025–1036.
11. Yunger S, Rosenfeld L, Garini Y, Shav-Tal Y (2010) Single-allele analysis of transcription kinetics in living mammalian cells. *Nat Methods* 7(8):631–633.
12. Larson DR, Zenklusen D, Wu B, Chao JA, Singer RH (2011) Real-time observation of transcription initiation and elongation on an endogenous yeast gene. *Science* 332(6028):475–478.
13. Lionnet T, et al. (2011) A transgenic mouse for in vivo detection of endogenous labeled mRNA. *Nat Methods* 8(2):165–170.
14. Forrest KM, Gavis ER (2003) Live imaging of endogenous RNA reveals a diffusion and entrapment mechanism for nanos mRNA localization in *Drosophila*. *Curr Biol* 13(14): 1159–1168.
15. Blackwood EM, Kadonaga JT (1998) Going the distance: A current view of enhancer action. *Science* 281(5373):60–63.
16. Pisarev A, Poustelnikova E, Samsonova M, Reinitz J (2009) FlyEx, the quantitative atlas on segmentation gene expression at cellular resolution. *Nucleic Acids Res* 37(Database issue):D560–D566.
17. Little SC, Tikhonov M, Gregor T (2013) Precise developmental gene expression arises from globally stochastic transcriptional activity. *Cell* 154(4):789–800.
18. Lionnet T, Singer RH (2012) Transcription goes digital. *EMBO Rep* 13(4):313–321.
19. Ludwig MZ, Manu, Kittler R, White KP, Kreitman M (2011) Consequences of eukaryotic enhancer architecture for gene expression dynamics, development, and fitness. *PLoS Genet* 7(11):e1002364.
20. Harding K, Hoey T, Warrior R, Levine M (1989) Autoregulatory and gap gene response elements of the *even-skipped* promoter of *Drosophila*. *EMBO J* 8(4):1205–1212.
21. Goto T, Macdonald P, Maniatis T (1989) Early and late periodic patterns of *even skipped* expression are controlled by distinct regulatory elements that respond to different spatial cues. *Cell* 57(3):413–422.
22. Shermoen AW, O'Farrell PH (1991) Progression of the cell cycle through mitosis leads to abortion of nascent transcripts. *Cell* 67(2):303–310.
23. Frasch M, Levine M (1987) Complementary patterns of *even-skipped* and *fushi tarazu* expression involve their differential regulation by a common set of segmentation genes in *Drosophila*. *Genes Dev* 1(9):981–995.
24. Edgar BA, Weir MP, Schubiger G, Kornberg T (1986) Repression and turnover pattern *fushi tarazu* RNA in the early *Drosophila* embryo. *Cell* 47(5):747–754.
25. Petkova MD, Little SC, Liu F, Gregor T (2014) Maternal origins of developmental reproducibility. *Curr Biol* 24(11):1283–1288.
26. Kellerman KA, Mattson DM, Duncan I (1990) Mutations affecting the stability of the *fushi tarazu* protein of *Drosophila*. *Genes Dev* 4(11):1936–1950.
27. Paré A, et al. (2009) Visualization of individual Scr mRNAs during *Drosophila* embryogenesis yields evidence for transcriptional bursting. *Curr Biol* 19(23): 2037–2042.
28. Sanchez A, Golding I (2013) Genetic determinants and cellular constraints in noisy gene expression. *Science* 342(6163):1188–1193.
29. Munsky B, Neuert G, van Oudenaarden A (2012) Using gene expression noise to understand gene regulation. *Science* 336(6078):183–187.
30. Chubb JR, Trcek T, Shenoy SM, Singer RH (2006) Transcriptional pulsing of a developmental gene. *Curr Biol* 16(10):1018–1025.
31. Lagha M, et al. (2013) Paused Pol II coordinates tissue morphogenesis in the *Drosophila* embryo. *Cell* 153(5):976–987.
32. Choi PJ, Cai L, Frieda K, Xie XS (2008) A stochastic single-molecule event triggers phenotype switching of a bacterial cell. *Science* 322(5900):442–446.
33. Buecker C, Wysocka J (2012) Enhancers as information integration hubs in development: Lessons from genomics. *Trends Genet* 28(6):276–284.
34. Krivega I, Dean A (2012) Enhancer and promoter interactions-long distance calls. *Curr Opin Genet Dev* 22(2):79–85.
35. Petesch SJ, Lis JT (2012) Overcoming the nucleosome barrier during transcript elongation. *Trends Genet* 28(6):285–294.
36. Reinitz J, Sharp DH (1995) Mechanism of *eve* stripe formation. *Mech Dev* 49(1-2): 133–158.
37. Levine M, Cattoglio C, Tjian R (2014) Looping back to leap forward: Transcription enters a new era. *Cell* 157(1):13–25.
38. Liu F, Morrison AH, Gregor T (2013) Dynamic interpretation of maternal inputs by the *Drosophila* segmentation gene network. *Proc Natl Acad Sci USA* 110(17):6724–6729.
39. Dubuis JO, Samanta R, Gregor T (2013) Accurate measurements of dynamics and reproducibility in small genetic networks. *Mol Syst Biol* 9:639.

Supporting Information

Bothma et al. 10.1073/pnas.1410022111

SI Text

SI Methods

Cloning and Transgenesis. A plasmid construct containing the *even-skipped* (*eve*) enhancer and promoter region (−1.7 kb, +50 bp) was built using the pbPHi backbone vector containing *yellow* reporter gene (1, 2). The *yellow* reporter gene (6.4 kb) was used instead of *lacZ* (5.3 kb) (3) to increase the signal strength, which is proportional to the length of the reporter. This is because the number of transcripts associated with the template is directly proportional to the length of the reporter when the MS2 repeats are placed in the 5′ position. Primers used for building the construct are atttgcggccgcCAAGAAGGCTTGCATGTGGG and cgggatccAACGAAGGCAGTTAGTTGTTGACTG. Copies of the MS2 stem loops were extracted from plasmid pCR4-24XMS2SL-stable (Addgene; 31865) by digesting it with BamHI and BglII restriction enzymes. This fragment was ligated into *eve-yellow* pbPHI vector linearized with BamHI. The *eve2*-MS2-yellow plasmid was integrated on chromosome 3 (Vk33).

In Situ Hybridization and Fluorescence Microscopy. Fluorescent in situ hybridization was performed as described previously using hapten-tagged complementary mRNA probes (4, 5). Embryos were imaged on a Zeiss 700 laser-scanning microscope in *z* stacks through the nuclear layer at 0.5-μm intervals using a Plan-Apochromat 20×/0.8 air lens.

Live Imaging Sample Preparation and Data Acquisition. Female virgins of line yw; Histone-RFP;MCP-NoNLS-GFP (3) were crossed with males of the reporter line (*eve2*-MS2-yellow). Collected embryos were dechorinated with bleach and mounted between a semipermeable membrane (Biofolie; In Vitro Systems & Services) and a coverslip and embedded in Halocarbon 27 oil (Sigma). Excess oil was removed with absorbent paper from the sides to flatten the embryos slightly. The flattening of the embryos makes it possible to image more nuclei in the same focal plane without causing any detectable change to early development processes (6).

Embryos were either imaged using a custom-built two-photon microscope (7) at Princeton and a Zeiss LSM 780 confocal microscope at University of California, Berkeley. On the two-photon microscope, imaging conditions were as described by Garcia et al. (3): average laser power at the specimen was 10 mW, a pixel size is 220 nm, and image resolution is 512 × 256 pixels. At each time point, a stack of 10 images separated by 1 μm was acquired, resulting in a final time resolution of 37 s. Confocal imaging on the Zeiss LSM 780 was performed using a Plan-Apochromat 40×/1.4 N.A. oil immersion objective. The MCP-GFP and Histone-RFP were excited with a laser wavelength of 488 and 561 nm, respectively. Fluorescence was detected with two separate photomultiplier tubes using the Zeiss QUASAR detection unit (gallium–arsenide–phosphide photomultiplier was used for the GFP signal, whereas the conventional detector was used for the RFP). Pixel size is 198 nm, and images were captured at 512 × 512 pixel resolution with the pinhole set to a diameter of 116 μm. At each time point, a stack of 22 images separated by 0.5 μm were captured, spanning the nuclear layer. The final time resolution is 32 s.

Live-Imaging Data Analysis. Analysis was performed as described in ref. 3. Histone-RFP slices were maximum projected for each time point. Nuclei were segmented using a blob detection approach based on the Laplacian of Gaussian filter kernel. The segmented nuclei were then tracked over multiple nuclear cycles. Initially, each time frame of the MCP-GFP channel is treated independently. Spots are detected in 3D using raw images and assigned to their respectively closest nucleus. When multiple spots are detected in the vicinity of the nucleus (due to segregating sister chromatids), only the brightest one is kept. When single traces are shown, the automated tracking of both nuclei and spots was checked manually frame by frame using custom analysis code. Spot intensity determination requires an estimate of the local fluorescent background for each particle. Two-dimensional Gaussian fits to the peak plane of each particle column determines an offset, which is used as background estimator. The intensity is calculated by integrating the particle fluorescence over a circle with a radius of 6 pixels and subtracting the estimated background. Imaging error is dominated by the error made in the fluorescent background estimation (3).

In ref. 3, it was possible to measure the average fluorescence per polymerase molecule for the *hunchback*>MS2 transgene with 24 MS2 repeats. The quantitative imaging for the *eve*>MS2 transgene was conducted under the exact same imaging conditions on the same microscope. The *eve*>MS2 transgene also possess 24 MS2 repeats. However, the specific sequence of the stem loops is slightly different as these repeats have been further optimized to facilitate molecular biology work with them (8). Assuming that the MS2 sites are similarly saturated in both cases, we can then use the average fluorescence per polymerase molecule calculated for the *hunchback*>MS2 transgene to calibrate the *eve*>MS2 fluorescent traces in terms of the absolute number of transcribing polymerases per fluorescent spot (Fig. 4). It is important, however, to point out that this is an estimate and that a direct calibration between fluorescence and MS2-*eve* transcripts will be necessary for further confidence.

We quantified expression domain refinement dynamics by fitting a Gaussian curve to the profile of the fraction of active nuclei as a function of anterior-posterior (AP) position at each time point in nuclear cycle 14 (nc14) (Fig. 2*D*, dashed line). The fits define an expression domain width over which we determined the instantaneous fraction of active nuclei. The width of the expression domain as well as the fraction of active nuclei refine into the mature stripe pattern during the initial 20 min of expression (Fig. 2*E*).

Determining the Amount of mRNA Accumulated in the Presence of Degradation. In the experiments reported here, the quantity that is measured is the observed fluorescence in foci of transcription, which is proportional to the number of nascent mRNA molecules associated with a locus at a specific time. This is related to, but not exactly equal to, the rate of mRNA production. One quantity that is of particular interest is how much mRNA has accumulated in individual cells at a specific time point. To connect the measured fluorescence to the amount of mRNA produced by a cell up to a given time, we have to obtain the rate of mRNA production from the fluorescence traces and then account for the corresponding mRNA degradation. In the following sections, we give details on how this magnitude is calculated. The first section describes how to connect the measured fluorescence with the rate of mRNA production, and the second describes how we to use the obtained mRNA production rate to estimate the amount of accumulated mRNA in the presence of degradation.

Relating Measured Fluorescence to mRNA Production Rate. The observed fluorescence in foci of transcription as a function of time is given by $F(t)$. This quantity is linearly related to the number of mRNA molecules associated with the DNA template at a given instant. In our model, mRNA molecules remain associated with the DNA template for as long as it takes the transcribing polymerase to traverse the length of the gene, E_t. Hence, after a time $(E_t + t)$, all of the mRNA associated with the active locus at a time t have been released from the template. Thus,

$$F(t) = \overline{N_p}(t + E_t) - \overline{N_p}(t),$$

where $\overline{N_p}(t)$ is the number of mRNAs that have been produced up to time point t, properly scaled by the average fluorescence intensity for a single mRNA molecule. Now, we can expand $\overline{N_p}(t + E_t)$ around $E_t/2$, which results in the following:

$$\overline{N_p}(t + E_t) = \overline{N_p}\left(t + \frac{E_t}{2} + \frac{E_t}{2}\right) = \sum_{n=0}^{\infty} \frac{\overline{N_p}^{(n)}\left(t + \frac{E_t}{2}\right)}{n!}\left(\frac{E_t}{2}\right)^n.$$

Similarly, we can expand $\overline{N_p}(t)$, obtaining the following:

$$\overline{N_p}(t) = \overline{N_p}\left(t + \frac{E_t}{2} - \frac{E_t}{2}\right) = \sum_{n=0}^{\infty} \frac{\overline{N_p}^{(n)}\left(t + \frac{E_t}{2}\right)}{n!}\left(-\frac{E_t}{2}\right)^n.$$

As a result,

$$\overline{N_p}(t + E_t) - \overline{N_p}(t) = \sum_{n=0}^{\infty} \frac{\overline{N_p}^{(2n+1)}\left(t + \frac{E_t}{2}\right)}{(2n+1)!}\left(\frac{E_t}{2}\right)^{2n+1}$$

$$= \frac{d\overline{N_p}}{dt}\left(t + \frac{E_t}{2}\right) \times \left(\frac{E_t}{2}\right) + \text{h.o.t},$$

where "h.o.t" indicates higher-order terms. This implies that

$$F(t) \approx \frac{d\overline{N_p}}{dt}\left(t + \frac{E_t}{2}\right) \times \left(\frac{E_t}{2}\right)$$

and

$$\frac{d\overline{N_p}(t)}{dt} \approx \frac{2}{E_t} \times F\left(t - \frac{E_t}{2}\right).$$

As a result, by integrating the measured fluorescence one can obtain, up to a multiplicative constant, the amount of mRNA produced as a function of time. The details on how this is done is detailed in the next section.

Relating mRNA Production Rate to Amount of mRNA Accumulated. In the previous section, we derived a connection between the measured fluorescence and the rate of mRNA production. In the absence of mRNA degradation and neglecting diffusion of mRNA between cells, the total amount of mRNA associated with a given nucleus at a given time is as follows:

$$\overline{N_{\text{mRNA}}}(t) = \int_0^t \frac{d\overline{N_p}(\tau)}{dt} d\tau.$$

If we have to allow for mRNA degradation according to first-order kinetics, this simply becomes the following:

$$\overline{N_{\text{mRNA}}}(t) = \int_0^t \left(\frac{d\overline{N_p}(\tau)}{dt} - \lambda \times \overline{N_{\text{mRNA}}}(\tau)\right) d\tau.$$

Hence, given some initial conditions and the rate of mRNA production estimated from our measurements, we can integrate the above equation to obtain the accumulated amount of mRNA present in a cell at a given time.

SI Discussion

Using the methods explained in the previous sections, it is possible to relate the measured fluorescence (Fig. S1*A*) to the amount of mRNA accumulated (Fig. S1*B*). Fig. S1*B* shows how the amount of accumulated mRNA changes with time when one assumes different half-lives. When the mRNA half-life is short, the accumulated amount of mRNA plateaus relatively soon into cell cycle 14 while it steadily increases with time for longer half-lives. The overall levels of mRNA accumulated also scales with the mRNA half-life. One of the things we wanted to get a sense of is how different half-lives of mRNA affect the qualitative profile of the stipe. To look at this, we determined the mRNA accumulation profile for a given embryo assuming different half-lives (Fig. S1 *C* and *D*, and Movie S5). Although there appears to be a modest increase in the width of the stripe as the mRNA half-life is increased, it is not a striking difference. Fig. S1*E* shows that increasing the mRNA half-life from 5 to 60 min only leads to a small increase in the number of cells on the boundary of the stripe even though the half-life is varied by more than an order of magnitude. Movie S5 does show how the persistence of mRNA increases as the mRNA half-life is increased. It is not clear how biologically relevant the persistence of the mRNA driven by stripe 2 enhancer is later because there is an autoregulatory enhancer that takes over from the eve 2 enhancer to drive expression later (9).

In this study, we have looked at the dynamics of mRNA accumulation. How this will connect to the dynamics of the protein distribution will depend strongly on the half-life of the eve protein in the early embryo. Although this has not been measured for eve, the half-lives of the ftz and engrailed proteins have been measured and both found to be short, <10 min (10, 11). Hence it is likely that the eve protein will have a lifetime on this order [also consistent with estimates from modeling work (12)]. With such a short half-life, the evolution of the protein pattern will be closely coupled to that of the accumulated mRNA pattern.

We relate the fluorescence dynamics to the rate of RNA polymerase II (Pol II) loading at the promoter by invoking a simple model previously used to analyze the mean transcriptional activity of multiple MS2 spots (3). In the following section, we describe the general idea of the models, how they are used to fit the data and extract the single-cell dynamics of transcriptional initiation.

A cartoon depicting one possible outcome in the context of a two-state promoter is shown in Fig. 4 *B–D*. Here, at time t_1 after mitosis Pol II molecules are loaded at a constant rate r. Because at this point in time the gene is devoid of Pol II molecules, the fluorescence will increase as more polymerases escape the promoter and are loaded onto the gene. If the transcriptionally active state persists for a time longer than the time required for the first Pol II molecule to reach the end of the gene [6.4 kbp, which take 4.2 ± 0.4 min to transcribe (3)], the number of Pol II molecules on the gene will reach steady state, resulting in a constant fluorescence signal. At time t_2, the promoter switches back to the OFF state and Pol II molecules are not further loaded at the promoter while those that have finished elongation fall off the gene, resulting in a steady decrease of fluorescence intensity. This whole process can be repeated with

different characteristic times resulting in the modulation of the burst size and frequency.

In a "multistate" transcription model (Fig. 4 *B–D*), the promoter can load Pol II molecules onto the gene a varying discrete rates. The result is more complex fluorescence dynamics, but the connection between the fluorescent signal and the rate of transcriptional initiation remains the same as in the case of the "two-state" transcription model.

Fits of the model to the fluorescence data to extract the dynamics of transcriptional initiation were performed manually using custom-written code in Matlab. It is important to point out that these fits should only be seen as an estimate of the dynamics. An unbiased algorithm to fit the data in an automated way is currently under development and will allow for the systematic characterization of these in vivo single-molecule data.

1. Venken KJT, He Y, Hoskins RA, Bellen HJ (2006) P[acman]: A BAC transgenic platform for targeted insertion of large DNA fragments in *D. melanogaster*. *Science* 314(5806): 1747–1751.
2. Perry MW, Boettiger AN, Bothma JP, Levine M (2010) Shadow enhancers foster robustness of *Drosophila* gastrulation. *Curr Biol* 20(17):1562–1567.
3. Garcia HG, Tikhonov M, Lin A, Gregor T (2013) Quantitative imaging of transcription in living *Drosophila* embryos links polymerase activity to patterning. *Curr Biol* 23(21): 2140–2145.
4. Bothma JP, Magliocco J, Levine M (2011) The snail repressor inhibits release, not elongation, of paused Pol II in the *Drosophila* embryo. *Curr Biol* 21(18):1571–1577.
5. Kosman D, et al. (2004) Multiplex detection of RNA expression in *Drosophila* embryos. *Science* 305(5685):846.
6. Di Talia S, Wieschaus EF (2012) Short-term integration of Cdc25 dynamics controls mitotic entry during *Drosophila* gastrulation. *Dev Cell* 22(4):763–774.
7. Liu F, Morrison AH, Gregor T (2013) Dynamic interpretation of maternal inputs by the *Drosophila* segmentation gene network. *Proc Natl Acad Sci USA* 110(17):6724–6729.
8. Hocine S, Raymond P, Zenklusen D, Chao JA, Singer RH (2013) Single-molecule analysis of gene expression using two-color RNA labeling in live yeast. *Nat Methods* 10(2): 119–121.
9. Harding K, Hoey T, Warrior R, Levine M (1989) Autoregulatory and gap gene response elements of the *even-skipped* promoter of *Drosophila*. *EMBO J* 8(4):1205–1212.
10. Edgar BA, Odell GM, Schubiger G (1987) Cytoarchitecture and the patterning of *fushi tarazu* expression in the *Drosophila* blastoderm. *Genes Dev* 1(10):1226–1237.
11. Kellerman KA, Mattson DM, Duncan I (1990) Mutations affecting the stability of the *fushi tarazu* protein of *Drosophila*. *Genes Dev* 4(11):1936–1950.
12. Jaeger J, et al. (2004) Dynamic control of positional information in the early *Drosophila* embryo. *Nature* 430(6997):368–371.

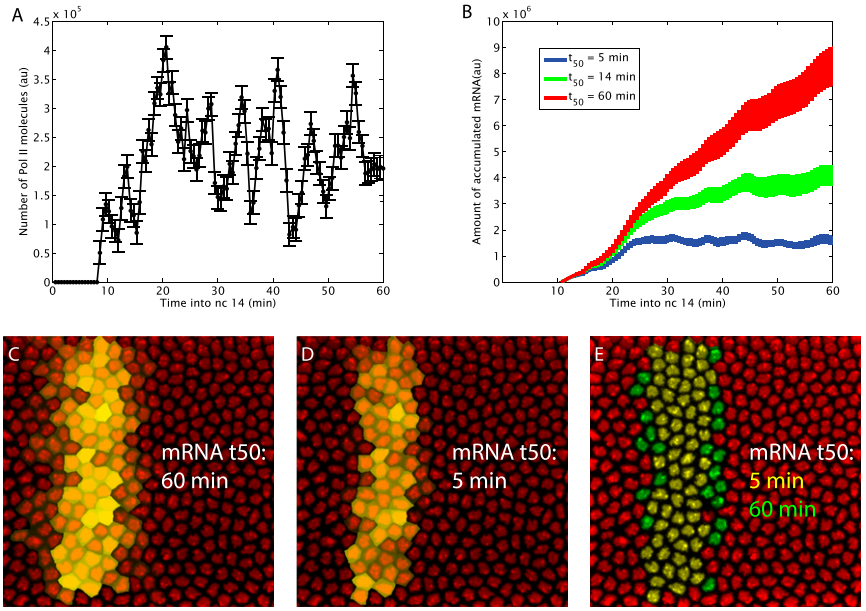

Fig. S1. Role of mRNA half-life on mRNA accumulation and profile of the stripe domain. (*A*) Fluorescence intensity as a function of time for an individual spot in the center of the *eve* expression pattern. (*B*) Calculated accumulated mRNA as a function of time for different mRNA half-lives. (*C* and *D*) Profile of the accumulated mRNA in an embryo when different half-lives are assumed, the false coloring of nuclei indicating the amount of mRNA produced. Each panel has been rescaled according to the maximum amount of mRNA accumulated during the course of the movie. (*E*) False-colored nuclei showing the stripe domain for 5- and 60-min half-lives. Nuclei were chosen to be within the stripe domain if they had an accumulated mRNA amount that was at least 25% of the maximum amount accumulated. [*A*, Error bars are imaging errors as in Garcia et al. (3); *B*, error bars are propagated from *A*; *C*, error bars correspond to the SEM over four embryos.]

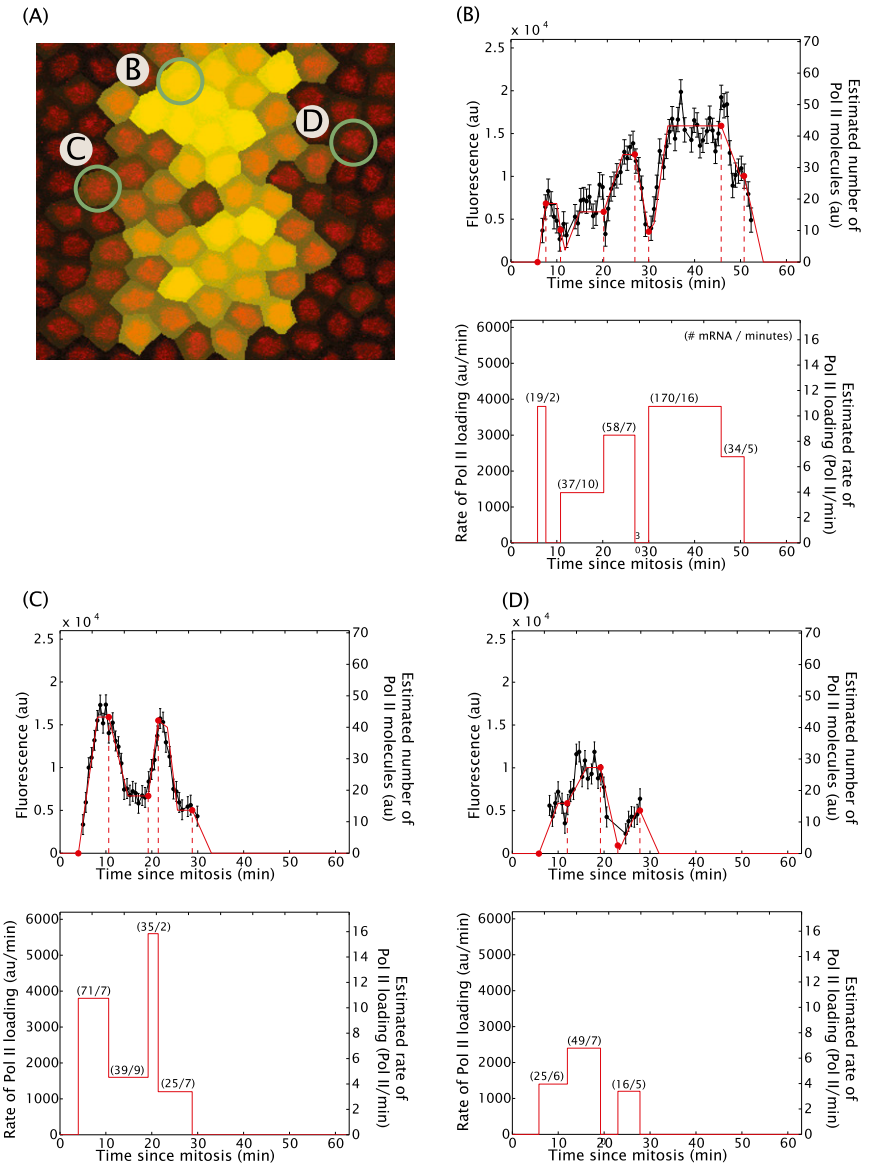

Fig. S2. Further evidence of transcriptional bursting in the *eve* stripe 2 domain. False coloring of nuclei indicating the amount of mRNA produced (Fig. 2 *D–F*). (*B–D*) Fluorescence intensity as a function of time for individual spots corresponding to the nuclei shown in *A* and estimated rate of Pol II loading resulting from manual fits as in Fig. 4. Note that transitions between multiple discrete states of transcription can be seen both inside and outside the mature stipe. The estimated number of mRNA molecules produced per state and their duration are shown. [Error bars are imaging errors as in Garcia et al. (3).]

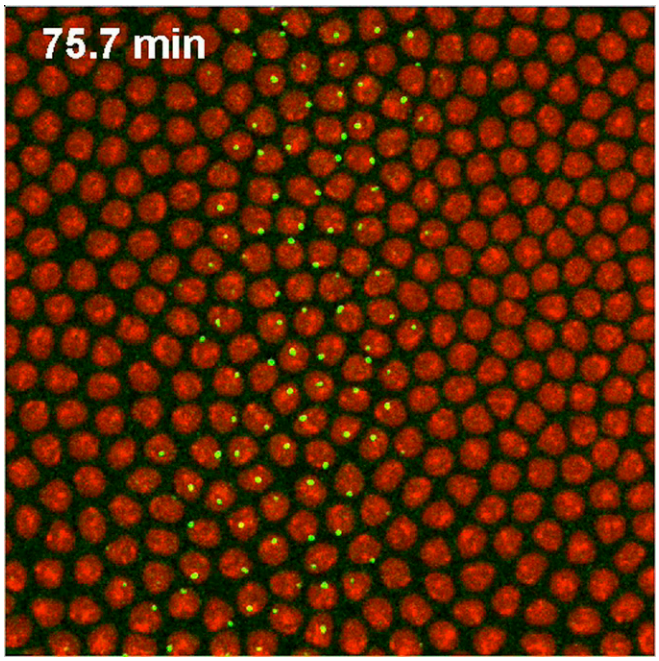

Movie S1. Dynamics of *eve* stripe 2 expression. Maximum projection of *eve*>MS2 transgene from nc11 to nc14 over 112 μm × 112-μm region centered on the stripe. Anterior is to the *Left*. The pattern is initially broad and gets refined during successive cell cycles to later on disappear at the onset of gastrulation. The snapshots from Fig. 1 are taken from this movie.

Movie S1

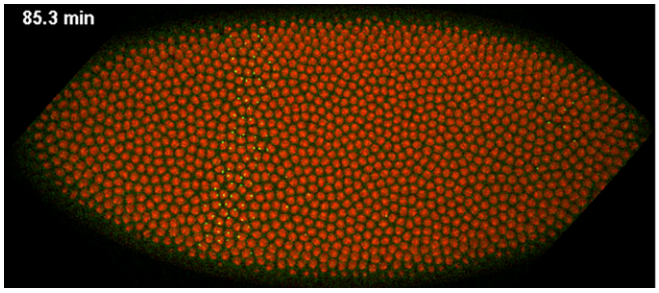

Movie S2. Whole-embryo dynamics of *eve* stripe 2 expression. Maximum projection of *eve*>MS2 transgene from end of nc10 to gastrulation for a whole embryo. Anterior is to the *Left*.

Movie S2

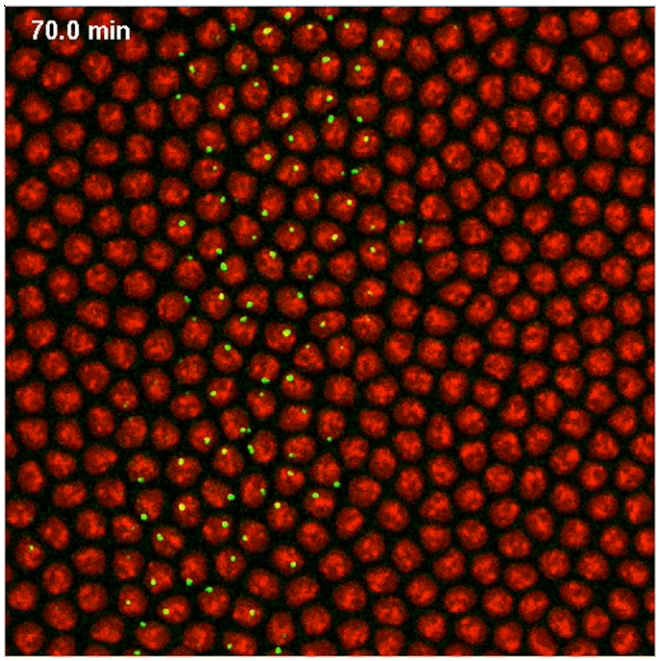

Movie S3. Further example of dynamics of *eve* stripe 2 formation. Maximum projection of *eve*>MS2 transgene from nc12 to nc14 over 112 μm × 112-μm region centered on the stripe. Anterior is to the *Left*. The pattern is initially broad and then gets refined during successive cell cycles and then the pattern eventually disappears.

Movie S3

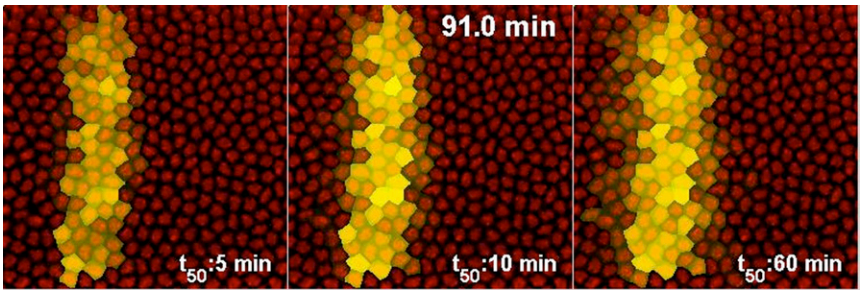

Movie S4. Effect of mRNA degradation on stripe formation. mRNA accumulation in the presence of degradation. The accumulated amount of mRNA per cell is shown as a function of time assuming different mRNA half-lives. The amount of accumulated mRNA is proportional to the degree of yellow false coloring. Because the absolute amount of mRNA accumulated is very different for different half-lives, each panel has been scaled according to the maximum accumulation reached during the course of each movie.

Movie S4

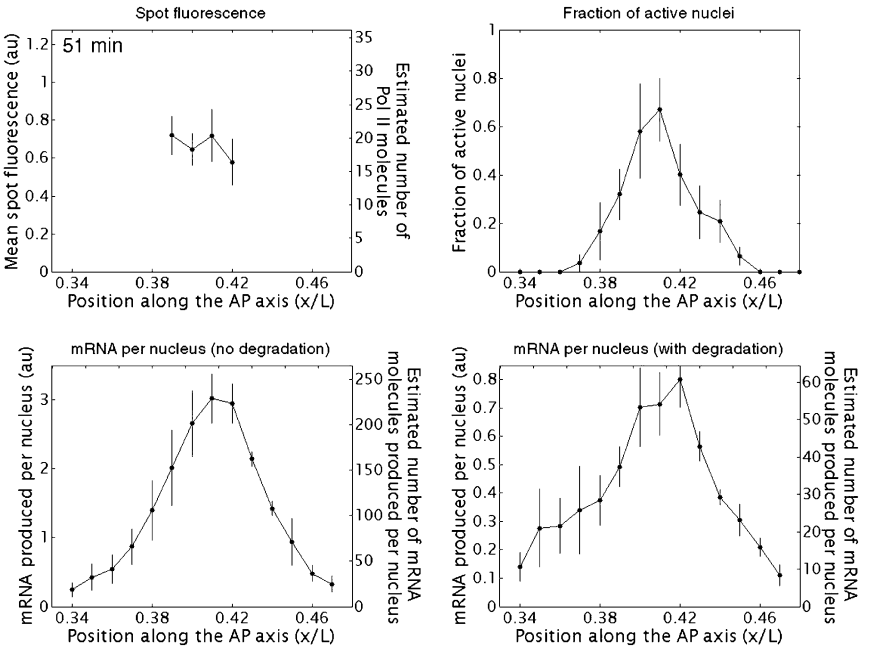

Movie S5. Quantitative dynamics of stripe formation and refinement. The mean spot fluorescence, instantaneous fraction of active nuclei, and accumulated amount of mRNA produced as a function of AP position are shown for different time points as in Fig. 3. The time stamp indicates time since the beginning of nc14. The mRNA produced us shown in the case of infinite half-life (mRNA accumulation) and of a half-life of 7 min. All data are obtained by averaging four different embryos. Error bars are SEM.

Movie S5